JJMIE

Volume 4, Number 1, Jan. 2010
ISSN 1995-6665
Pages 177- 192

Jordan Journal of Mechanical and Industrial Engineering

# Solar Net Collective Flux and Conversion Efficiency of the Nickel-Pigmented Aluminium Oxide Selective Absorber Prepared by Alternate and Reverse Periodic Technique in Different Prototype Volumes

A. Wazwaz [a, *], J. Salmi [b], R. Bes [c]

[a] *Department of Chemical Engineering, College of Engineering, Dhofar University, P.O.Box 2509, Postal Code 211, Salalah, Sultanate of Oman.*

[b] *Marion Technologies Nanomaterials, Nanostructured Materials & Ceramic Powders, Cap Delta - Parc Technologique Delta Sud, F-09340, Verniolle, France*

[c] *CIRIMAT/LCMIE, Université Paul Sabatier, 31062 Toulouse Cedex 4, France*

.

**Abstract**

Different constructed prototypes of different volumes were used to test different nickel- pigmented aluminium oxide selective absorber samples for photo thermal conversion. Different types of solar net collective flux (average, accumulative, maximum, minimum) were calculated. We found that there is a good linear mathematical relationship between the solar net collective fluxes with the prototype volume in the range 500 – 8000 ± 1 $cm^3$. Comparison between aluminium alloy, copper sheet, and the nickel-pigmented aluminium oxide selective absorber for net collective flux with nickel content and prototype volume were done. The highest net collective flux is for the sample of nickel content 60μg/$cm^2$ where: during a day, the accumulative net collective flux is 5586±1 W/$m^2$; while the average net collective flux is 372.4±0.1 W/$m^2$ in prototype of volume 500±1 $cm^3$. The lowest net collective flux is for the sample of nickel content 92μg/$cm^2$, where: during a day, the accumulative net collective flux is 4393±1 W/$m^2$; the average net collective flux is 292.9±0.1 W/$m^2$ in prototype of volume 8000±1 $cm^3$ .The percent conversion efficiency and absorption of merit are constants for all samples in all prototypes. The maximum average percent conversion efficiency is for sample of nickel content 60μg/$cm^2$ which lies in the range (72.0-74.0±0.1) %. However the least average percent conversion efficiency is for the sample of nickel content 92μg/$cm^2$ which lies in the range of (61.0-69.0±0.1) %. The best mathematical relations between the net collective flux and prototype volume were calculated. The correlation coefficients squared for all calculations are 0.91 on average.



Keywords: Selective Absorber; Nickel-Pigmented Aluminium Oxide, Prototype, Net Collective Flux, Conversion Efficiency, Absorption of Merit.

## 1. Introduction

Solar energy is an important, cheapest, and safe source of renewable energy. Therefore, it plays an important role in many different branches of our life. Solar energy materials are used commercially for photothermal, photoelectric energy production and for achieving energy efficiency in buildings. Developments in architecture with buildings are achieved using electrochromic and thermotropic windows. In agriculture, growths of plants are affected by being tuned to the spectral sensitivity for photosynthesis. The solar energy source is electromagnetic radiations that interact with matter.

We can utilize the solar energy by means of collectors. These collectors may be flat [12] or concentrating.

There are four basic types of concentrating collectors:

1. Parabolic trough [15].
2. Parabolic dish.
3. Power tower.
4. Stationary concentrating collectors.

The main part of the collector is the absorber. The absorber can be selective [1, 2] or non-selective, black or colored [3].

Selective surfaces/films/coatings form the basis of a wide range of very useful optical coatings and interference filters. Many fields such as chemistry, physics, and

* Corresponding author. arefwazwaz@hotmail.com.

technology are used to develop the optical coatings scientifically and industrially.

The selective coating may be ideal or non-ideal. The selectivity depends on the application we interested in [4, 11, 14].

The collector can be glazed, unglazed, or insulated. The glazed, insulated collector with absorber, which is selective, gives the best solar thermal performance. In our study the selective absorber is the nickel-pigmented aluminium oxide selective absorber.

We studied the optical properties (Absorptance, Reflectance, and Transmittance) of nine samples of nickel-pigmented aluminium oxide selective absorber, environmental conditions, and the configuration of our system (prototype) on the heating power and the conversion efficiency [5] of the selective absorber.

The cover used is a commercial polyethylene, because it reduces the convective loss, of low cost, flexible and can protect the selective absorber from degradation caused by exposing the absorber directly to the environment.

The performance of the flat-plate collector with an absorber for photothermal conversion can be described by the conversion efficiency ($\eta$) [13]. The conversion efficiency depends on the collective flux which in turn depends on the radiation flux and the heat loss. The radiation losses can be calculated using the Stefan-Boltzmann law and the other losses can be easily calculated, because they are dependent on the configuration and environment of the system. These losses are also linearly proportional to the temperature.

The effective role of the selective absorbers in photothermal conversion can be described by two cases. Both of them are concerned with the calculation of the collector efficiency. One is where the conduction and convection losses are assumed to be negligible compared to the radiation losses. This is also valid if the collector is operating at a high temperature. To maximize the conversion efficiency for both flat-plate and concentrating collectors, the loss of heat must be reduced while the absorptance-transmittance product must be increased to be close to unity. The performance of photothermal converters is also dependent on absorptivity ($\alpha$) and emissivity ($\varepsilon$) separately.

The second case is where the conduction and convection losses are not neglected. These losses are strongly dependent on the environment (wind velocity, humidity, ambient temperature) and on the configuration of the systems [6].

Many scientists have discussed the thermodynamic equations governing the efficiency of solar collectors. Advances and development in fundamental physics and chemistry can lead to new and more efficient solar energy materials that have very widespread applications [6-8].

In this paper we study the relationship between the net collective fluxes (average, accumulative, and maximum), percent conversion efficiency, and absorption of merit with nickel content and the prototype volume.

## 2. Experimental

The constructed models were tested outdoors during daylight under clear sky at Bethlehem University from June to October. All measurements are done at steady state conditions. The selective absorbers were put on a horizontal plane. The experimental model for the flat-plate collector (prototype) is consisting of the selective absorber, the insulated box, the transparent cover, and the data logger.

### *2.1. Selective Absorber*

Nickel-pigmented alumina was prepared on aluminium alloy substrate. Samples of different optical properties were used. These samples were prepared using an electrochemical process. Anodic aluminium (alumina) was first formed followed by pigmentation of alumina by nickel using alternate or reverse periodic current.

Scanning electron microscopy was used to determine the structure of the selective absorber surface and the thickness of the coatings. The thickness measured was found to be in the range from 0.350 to 0.400 μm.

The optical properties (hemispherical absorptivity $\alpha$ and hemispherical emissivity $\varepsilon$) were measured using an absorptiometer (EL 510 Elan Informatique) and an emissiometer (EL 520 Elan Informatique) at 70$^{o}$C, respectively. X-ray diffraction was used to test the presence of impurity phases [5].

The following block diagram illustrates preparation of aluminium alloy surface.


Figure 1. The electrochemical cell for the anodization of aluminium alloy.

The pigmentation of alumina with nickel was done using alternate and reverse periodic currents [5].
The schematic of the resulted layers from anodization and pigmentation is shown in Figure 2.

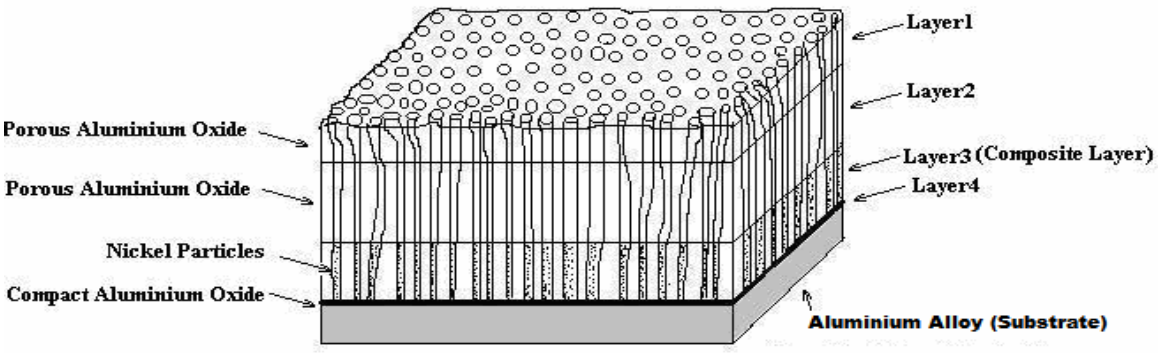


Figure 2. Schematic of the cross-section of the prepared selective absorber.

*2.2. Insulated Box (Prototype).*

Four different types (by volume) of prototypes were used. Figure 3 illustrates schematically the structure of the prototype. Table1 gives the dimensions for each prototype.

Table1. Dimensions of the prototypes used in the solar thermal performance.

| Box type | Length(cm)xWidth(cm)x Height(cm) | Volume ($\pm$1cm$^3$) | Shield Area ($\pm$1cm$^2$) |
|---|---|---|---|
| A | 10x10x5 | 500 | 100 |
| B | 15x15x5 | 1125 | 225 |
| C | 20x20x5 | 2000 | 400 |
| D | 40x40x5 | 8000 | 1600 |

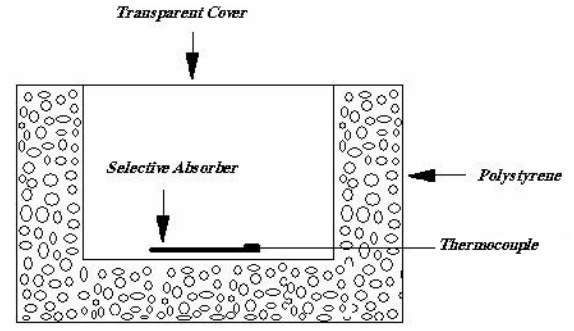


Figure 3. Schematic drawing of the prototype.

*2.3. The Transparent Cover*

A commercial polyethylene shield of thickness 50 µm and average transparency of 0.80 (in the solar range) was used. It is usually used to reduce the heat loss and to protect the absorber from degradation caused by exposing the absorber directly to the environment.

*2.4. The data logger*

The data logger used was HANDY-LOG DB-525 version 4 with DB-Lab WINDOWS$^{TM}$ software. This data logger is coupled with temperature sensors DT013 of temperature range -25$^o$C to 125$^o$C ($\pm$0.01$^o$C). In addition to, it is equipped with a relative humidity sensor (DT 041). The temperature of the selective absorber, the temperature Inside and outside the box, and the relative humidity were measured at the same time.

All the set-up components for the solar net collective flux (net heating power) measurements are shown in Figure 4.

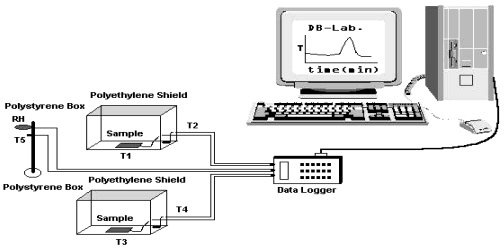


Figure 4. Schematic of all set-up components for the solar net collective flux measurements.

## 3. Method of Calculations

The performance of the selective absorber for photo-thermal conversion can be described by the conversion efficiency (η) which is defined as [6]:

$$\eta = \frac{\text{Energy extracted from the system}}{\text{Energy input}} = \frac{Ee}{A\,Is} \qquad (1)$$

Where
A is the area of the absorber exposed to the flux.
$I_s$ is the incident flux. $E_e$ is the extracted energy from the system (also, called net collective flux or net heating power).

$E_e$ = (Energy absorbed) - (Energy lost)

$$E_e = (t\alpha)\,A\,I_s - U_L \qquad (2)$$

Where tα is the effective transmittance-absorptance coefficient product for a single covered collector.
t is the transmittance of the cover. $U_L$ is the overall loss of energy from the absorber. $U_L$ is the sum of three parameters that involved in the heating process, namely, radiation, conduction, and convection losses.

The radiation losses can be calculated using Stephan-Boltzmann law and the other losses are dependent on the configuration and environment of the system. Moreover, these losses are linearly proportional to the temperature.

The effective role of the selective absorbers in photo-thermal conversion can be described by two cases. Both of them are concern with the calculation of the collector efficiency.

The first case is where the conduction and convection losses are assumed to be negligible compared to the radiation losses. It is also valid if the collector is operating at high temperatures. In this case the extracted energy (heating flux, $E_e$) can be calculated as in the following relation:

$$E_e = (t\alpha)\, A\, I_s - \sigma A \epsilon\, (T_s^4 - T_a^4) \qquad (3)$$

Where
A is the area of the absorber.
σ is Stephan-Boltzmann constant ($5.678\ 10^{-8}$ W.m$^{-2}$ K$^{-4}$).
Є is the thermal emittance at temperature Ts of the absorber.
$T_a$ is the temperature of the ambient.
$T_s$ is the temperature of the selective absorber.
The conversion efficiency (η) becomes:

$$\eta = t\alpha - \frac{\sigma\varepsilon(Ts^4 - T^4 a)}{Is} \qquad (4)$$

If the absorber is illuminated with a concentrated solar flux of concentration ratio X, then relation 4 becomes:

$$\eta = t\alpha - \frac{\sigma\varepsilon\,(Ts^4 - T^4 a)}{XIs} \qquad (5)$$

To maximize η for both flat plate and concentrating collectors, $U_L$ must be reduced while the absorptance-transmittance product must be increased to be close to unity.
The performance of photo-thermal converters is also depending on absorptivity (α) and emissivity (Є) separately. Therefore, the term absorptance of merit ($\alpha_m$) [6] was used to indicate the conversion efficiency (η) when there is no cover (t=1). It gives the upper limit for the conversion efficiency of a solar converter.

The output heat can be measured in terms of the mechanical work by using the Carnot efficiency which can be calculated for a particular reversible thermodynamic cycle as:

Where
W is the output work. $Q_s$ is the heat of the selective absorber.

$$\eta(\text{Carnot}) = \frac{W}{Qs} = \frac{Qs-Qa}{Qs} = \frac{Ts-Ta}{Ts} \qquad (6)$$

$T_s$, $T_a$ are the temperatures of the selective absorber and ambient; respectively.
The second case is where the conduction and convection losses are not neglected. In this case the extracted heating energy (Ee) (net collective flux or net heating power) can be calculated as

$$E_e = (t\alpha)I_s - B(T_s - T_a) - \sigma\epsilon_{eff}\,(T_s^4 - T_a^4) \qquad (7)$$

Where

B is the conduction-convection loss coefficient.

$\epsilon_{eff}$ is the effective emittance of the absorber and the atmosphere [9] which is given by:

$$\in_{eff} = \left[ \frac{1}{\in_s} + \frac{1}{\in_a} - 1 \right]^{-1} \qquad (8)$$

Where
$Є_s$ is the average emissivity of the selective absorber and
$Є_a$ is the average atmospheric emissivity.
The experimental model for testing the selective absorber consisting of: the insulated box, the transparent cover and the data logger are discussed in the previous section.
In addition to, the heat capacity of the system and the conduction-convection coefficient (B), for each prototype, were determined and used from previous study [5]. We wrote computer software to do all the calculations [5]

## 4. Results and Discussion

The relation between the accumulative and average net heating power (net collective flux) with prototype volume for aluminium alloy is shown in figure 5.
Linear regression for the accumulative and average net heating power for aluminium alloy gives the following relations:
Pac = -0.0291 V + 874.8 with $R^2 = 0.97$
Pav = -0.0019 V + 58.4 with $R^2 = 0.97$
Where
$\mathbf{P_{ac}}$ is the accumulative net heating power per square meter of aluminium alloy during a day.
$\mathbf{P_{av}}$ is the average net heating power per square meter of aluminium alloy per hour during a day.
**V** is the volume of the prototype in cubic centimeter. $\mathbf{R^2}$ is the correlation coefficient square.
These relations represent the accumulative and average net heating power for aluminium alloy; respectively.
The accumulative net collective flux is 874.8 W/m$^2$ and the average net collective is 58.4 W/m$^2$ when heat loss is neglected (V = 0.0 cm$^3$).
In addition to, we can do the same calculations for copper sheet. The comparison between aluminium alloy and copper sheet substrates is shown in figure 6.
As we see from figure 6, copper sheet has higher net collective flux (net heating power) by approximately one and half more than that of aluminium alloy. Therefore, copper sheet is a better substrate; this because copper has greater thermal conductance than aluminium alloy.
The effect of prototype volume on using nickel pigmented anodized aluminium selective absorber instead of aluminium alloy substrate is shown in the following tables and figures.
The variation of **Ts, Ta, ΔT, P, η** and $\boldsymbol{\alpha_m}$ with day time for nickel pigmented anodized aluminium selective absorber sample of nickel content 82 μg/cm$^2$ ,inside prototype A, is shown in table 2.

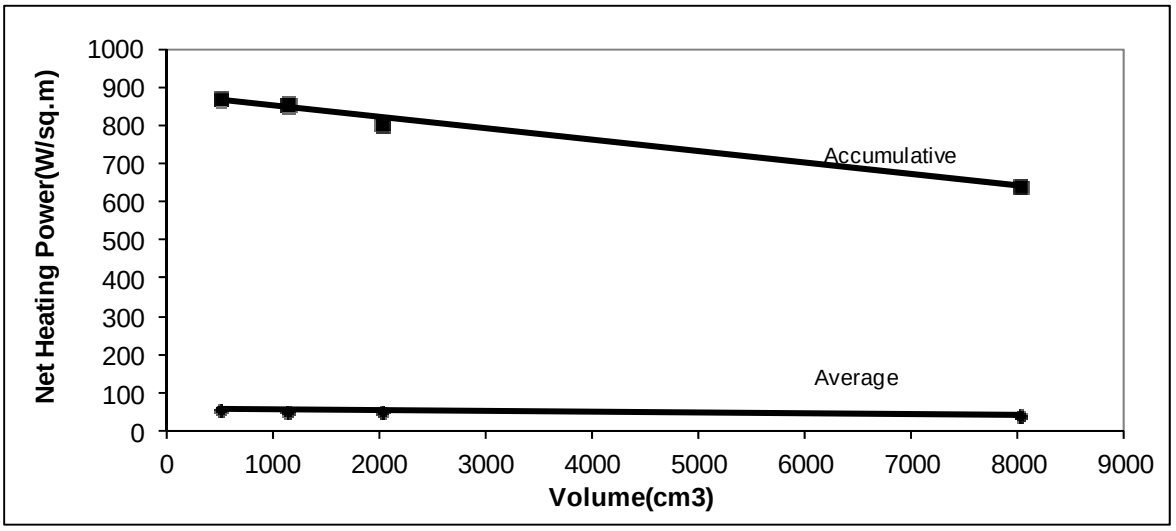


Figure 5. Variation of accumulative and average net heating power for aluminium alloy with prototype volume.

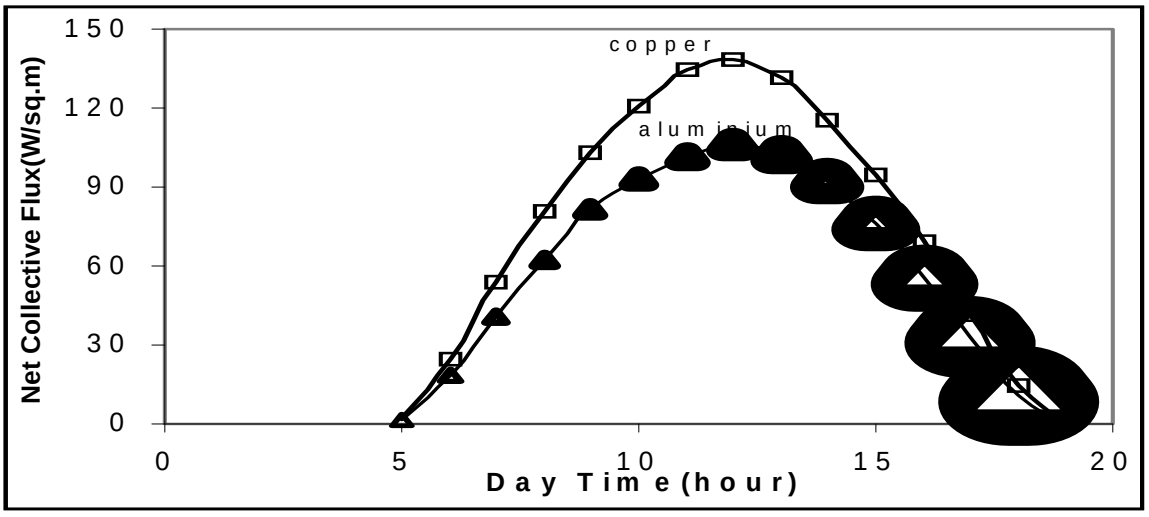


Figure 6. Variation of the net collective flux with the day time for aluminium alloy and copper sheet.

Table 2.Variation of Ts, Ta, ΔT, P, η and $\alpha_m$ with day time for selective absorber sample of nickel content 82 μg/cm$^2$ using prototype A.

| Time(h) | Ts($^o$C) (±0.01) | Ta($^o$C) (±0.01) | ΔT($^o$C) (±0.01) | P(W/m$^2$) (±0.01) | η (±0.01) | $\alpha_m$ (±0.01) | RH (%) (±0.01) |
|---|---|---|---|---|---|---|---|
| 5.00 | 24.82 | 23.54 | 1.28 | 16.02 | 0.76 | 0.96 | 33.47 |
| 6.00 | 24.66 | 23.06 | 1.60 | 119.68 | 0.77 | 0.96 | 37.25 |
| 7.00 | 29.79 | 27.55 | 2.24 | 264.01 | 0.77 | 0.96 | 34.73 |
| 8.00 | 37.00 | 30.31 | 6.69 | 399.58 | 0.77 | 0.96 | 24.20 |
| 9.00 | 46.00 | 32.51 | 13.49 | 506.54 | 0.77 | 0.96 | 24.04 |
| 10.00 | 64.86 | 31.87 | 32.99 | 600.94 | 0.76 | 0.96 | 33.32 |
| 11.00 | 68.07 | 29.79 | 38.28 | 656.57 | 0.76 | 0.96 | 39.76 |
| 12.00 | 35.72 | 29.31 | 6.41 | 667.63 | 0.77 | 0.96 | 41.17 |
| 13.00 | 32.83 | 28.83 | 4.00 | 639.42 | 0.77 | 0.96 | 44.48 |
| 14.00 | 30.75 | 28.03 | 2.72 | 571.94 | 0.77 | 0.96 | 46.68 |
| 15.00 | 30.11 | 27.55 | 2.56 | 459.82 | 0.77 | 0.96 | 46.68 |
| 16.00 | 29.31 | 26.91 | 2.40 | 340.03 | 0.77 | 0.96 | 47.46 |
| 17.00 | 28.19 | 26.11 | 2.08 | 204.12 | 0.77 | 0.96 | 47.46 |
| 18.00 | 27.07 | 24.82 | 2.25 | 68.17 | 0.77 | 0.96 | 50.60 |
| 19.00 | 25.79 | 23.70 | 2.09 | 0.00 | 0.00 | 0.79 | 54.85 |

From table 2:

Accumulative net collective flux (accumulative net heating power) is 5403±1 W/m$^2$.

Average net collective flux (average net heating power) is 360.2±0.1 W/m$^2$.

Average conversion efficiency is 69.0±0.1 %. Average absorption of merit is 95.0±0.1 %.

Average relative humidity is 40.4±0.1%.

The effect of adding the selective coating (nickel pigmented alumina), in comparison with aluminium alloy substrate, on the net collective flux (using prototype A) is shown in figure 7.

As we see from figure 7, adding the nickel pigmented anodized aluminium layer over the substrate will increase the net collective flux approximately eight times greater than that of using aluminium alloy alone.

In all measurements, we found that the maximum net collective flux obtained during a day is in the time interval 11:00AM to 13:00PM.

The behavior of sample of nickel content 82 μg/cm$^2$ compared with aluminium alloy substrate using prototype B is shown in figure 8.

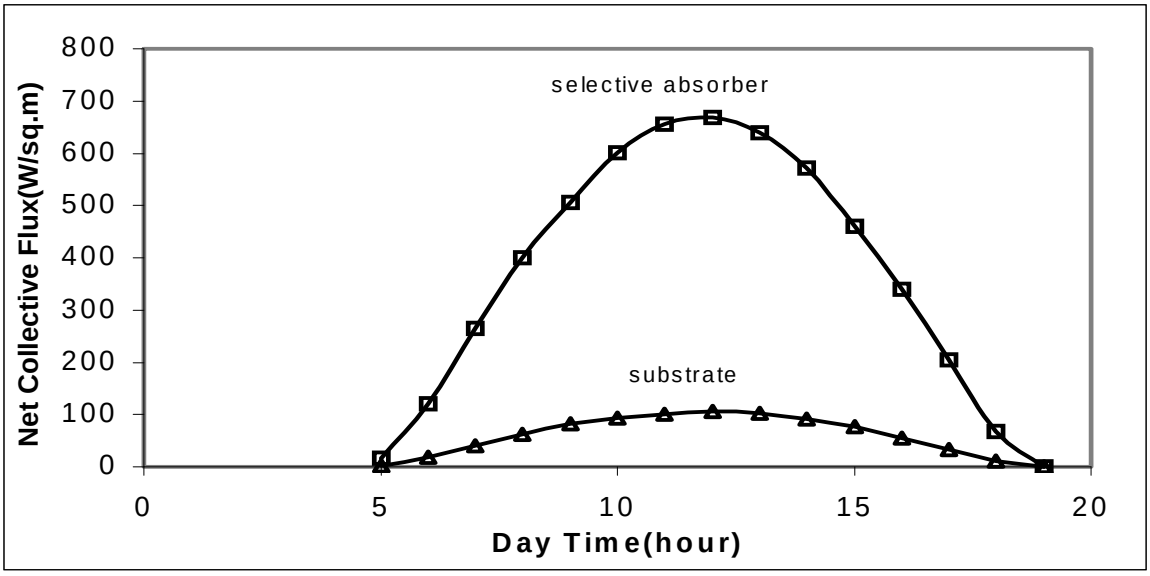


Figure 7. Effect of adding nickel pigmented anodized aluminium layer over aluminium alloy substrate on the net collective flux using prototype A.

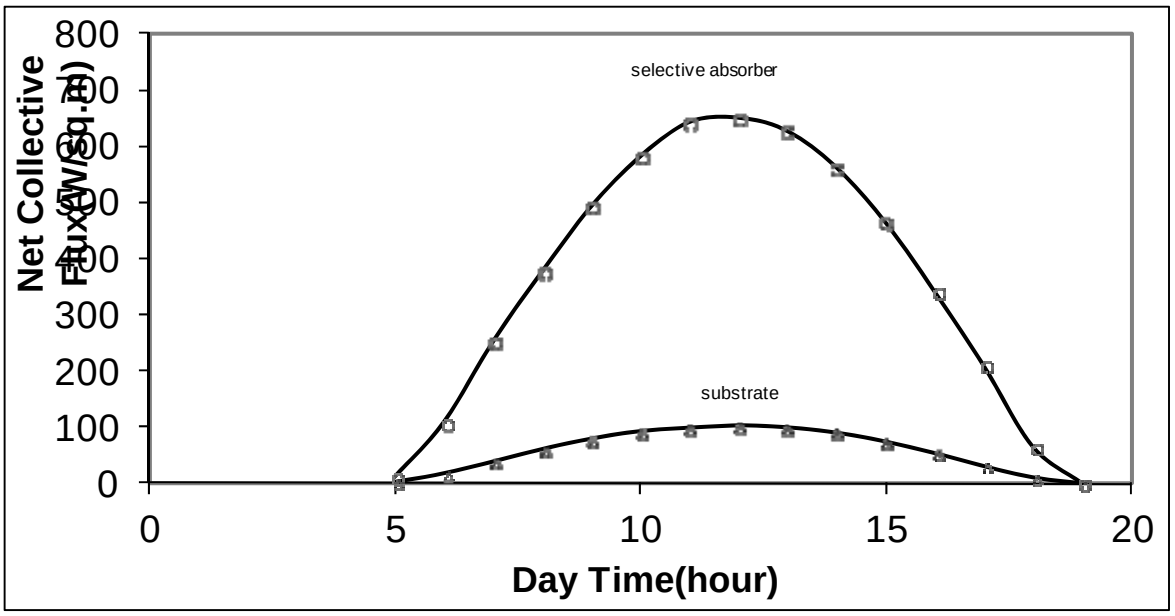


Figure 8. Variation of net collective flux with day time for selective absorber sample of nickel content 82 μg/cm$^2$ and aluminium alloy substrate using prototype B.

Comparing figure 8 with figure 7, prototype B gives less net collective flux than prototype A. This is because the conduction-convection and radiation losses are increased by increasing the prototype volume.

The same behavior will be obtained if we use prototypes C and D , but with less net collective flux during the day. The behavior of sample of nickel content 82 μg/cm$^2$ compared with the aluminium alloy during a day light inside prototype C is shown in figure 9.

Less net collective flux is obtained for both samples of nickel content 82 μg/cm$^2$ and the aluminium alloy substrate using prototype C.

However, using prototype D gives the same behavior but with less net heating power during a day because of the increase in the conduction-convection and radiation losses as we will see in table 3. Average relative humidity is 37.9±0.1%.

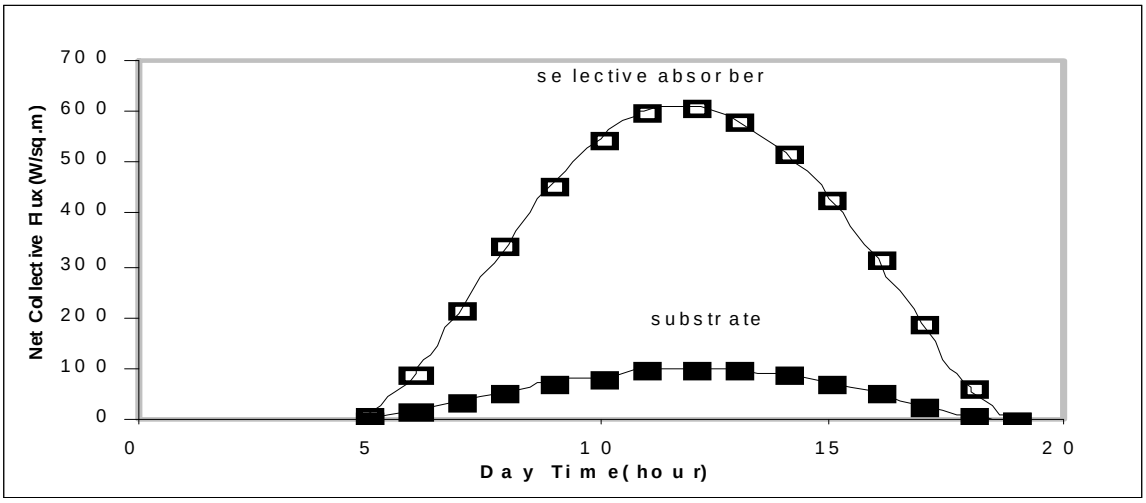


Figure 9. Variation of net collective flux with day time for selective absorber sample of nickel content 82 μg/cm$^2$ and aluminium alloy substrate using prototype C.

Table 3. Variation of Ts, Ta, ΔT, P, η and $\alpha_m$ with day time for selective absorber sample of nickel content 82 μg/cm$^2$ using prototype D.

| Time(h) | Ts($^o$C) (±0.01) | Ta($^o$C) (±0.01) | ΔT($^o$C) (±0.01) | P(W/m$^2$) (±0.01) | η (±0.01) | $\alpha_m$ (±0.01) | RH (%) (±0.01) |
|---|---|---|---|---|---|---|---|
| 5.00 | 27.07 | 27.07 | 0.00 | 0.00 | 0.00 | 0.96 | 38.50 |
| 6.00 | 27.23 | 27.23 | 0.00 | 60.67 | 0.77 | 0.96 | 38.82 |
| 7.00 | 28.35 | 27.55 | 0.80 | 184.91 | 0.76 | 0.96 | 37.72 |
| 8.00 | 35.23 | 35.07 | 0.16 | 331.59 | 0.77 | 0.96 | 30.33 |
| 9.00 | 56.62 | 42.12 | 14.50 | 436.01 | 0.74 | 0.93 | 24.83 |
| 10.00 | 73.99 | 38.44 | 35.55 | 504.87 | 0.71 | 0.90 | 26.25 |
| 11.00 | 69.51 | 37.64 | 31.87 | 561.43 | 0.72 | 0.91 | 28.76 |
| 12.00 | 41.64 | 34.43 | 7.21 | 606.66 | 0.76 | 0.95 | 34.73 |
| 13.00 | 39.08 | 33.95 | 5.13 | 580.70 | 0.76 | 0.95 | 35.36 |
| 14.00 | 37.48 | 33.79 | 3.69 | 505.60 | 0.76 | 0.95 | 35.99 |
| 15.00 | 36.04 | 33.63 | 2.41 | 394.21 | 0.76 | 0.95 | 37.56 |
| 16.00 | 35.07 | 32.51 | 2.56 | 271.92 | 0.76 | 0.95 | 46.99 |
| 17.00 | 33.15 | 31.39 | 1.76 | 135.40 | 0.76 | 0.95 | 50.45 |
| 18.00 | 31.71 | 30.43 | 1.28 | 23.07 | 0.72 | 0.91 | 50.60 |
| 19.00 | 30.27 | 29.47 | 0.80 | 0.00 | 0.94 | 0.02 | 52.02 |

Figures 8, 9 and 10 show that as the prototype volume increased (from A to D), the net collective flux is decreased during the day since the conduction-convection (B) and the radiation losses are increased. However, the nickel pigmented layer on aluminium alloy increases the net collective flux by approximately eight times in comparison with the aluminium alloy alone.

The behavior is the same in figures 8 to 10 for all nickel pigmented anodized aluminium selective absorber samples, but with different numerical results.

The variation of percent conversion efficiency with day time for sample of nickel content 82 μg/cm$^2$, using prototype A, is shown in figure 11.

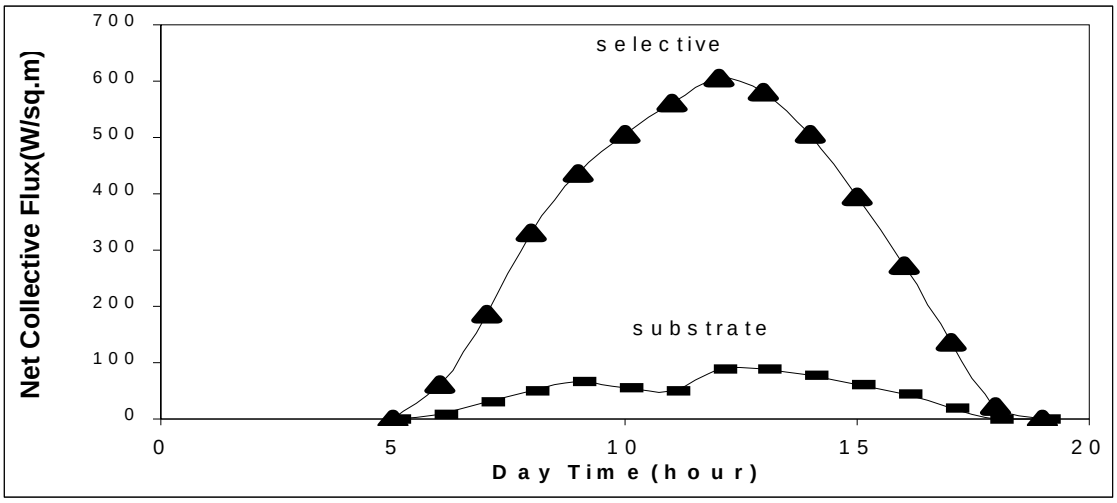


Figure 10. Variation of net collective flux with day time for sample of nickel content 82 μg/cm$^2$ and aluminium alloy substrate using prototype D.

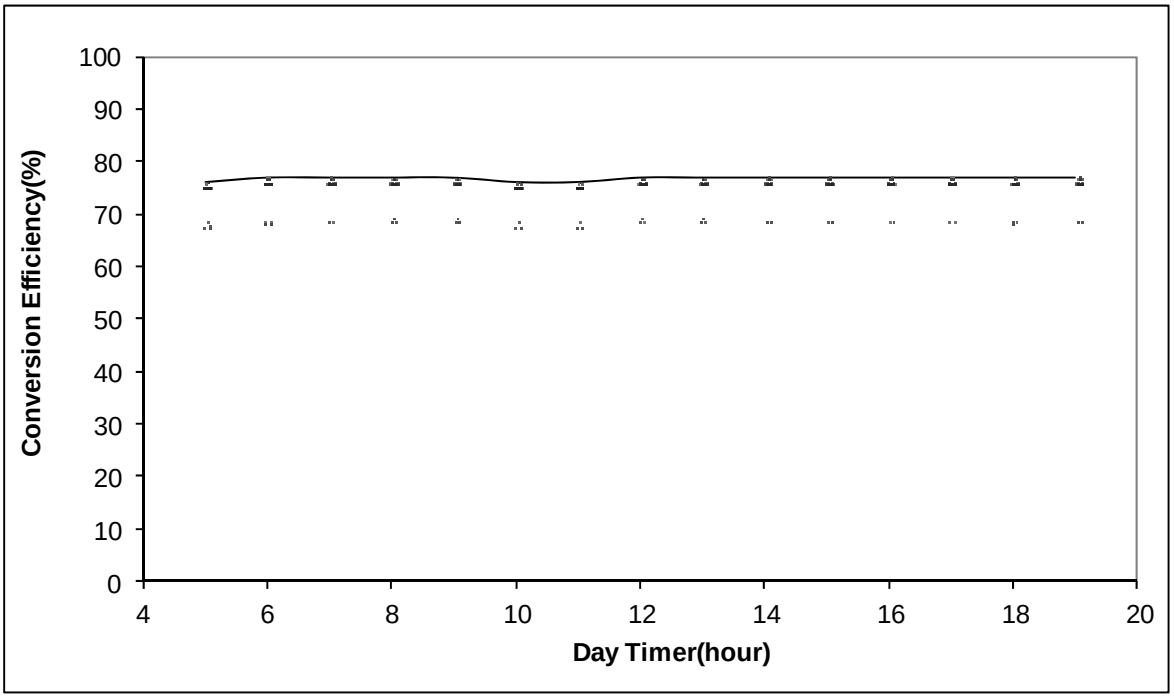


Figure 11. Variation of percent conversion efficiency as a function of day time for selective absorber sample of nickel content 82 μg/cm$^2$ using prototype A.

From figure 11, the percent conversion efficiency is constant during the day and this behavior is the same for all selective absorber samples using all prototypes, because the conversion efficiency depends, mainly, on the optical property of the sample.

The behavior of the percent absorption of merit during a day light for selective absorber sample of nickel content 82 μg/cm$^2$ using prototype A is shown figure 12.

As we see from figure 12, the percent absorption of merit is constant during a day and this is the same behavior for all other samples in all different prototypes, but with different numerical results. Absorption of merit depends, mainly, on the optical properties of the selective absorber sample and does not on the shield. It represents the maximum conversion efficiency that can be obtained if there is no shield on the prototype.

The accumulative net collective flux results for selective absorbers including copper sheet and aluminium alloy substrates are summarizes in table 4. These results represent all types of prototypes used.

Table 4 shows that the highest accumulative net collective flux (per day) is obtained using the selective absorber sample of nickel content 60μg/cm$^2$ which gives 5586±1W/m$^2$ in prototype A ; while the lowest value obtained with the selective absorber sample of nickel content 92μg/cm$^2$ which gives 4393±1W/m$^2$ in prototype D.

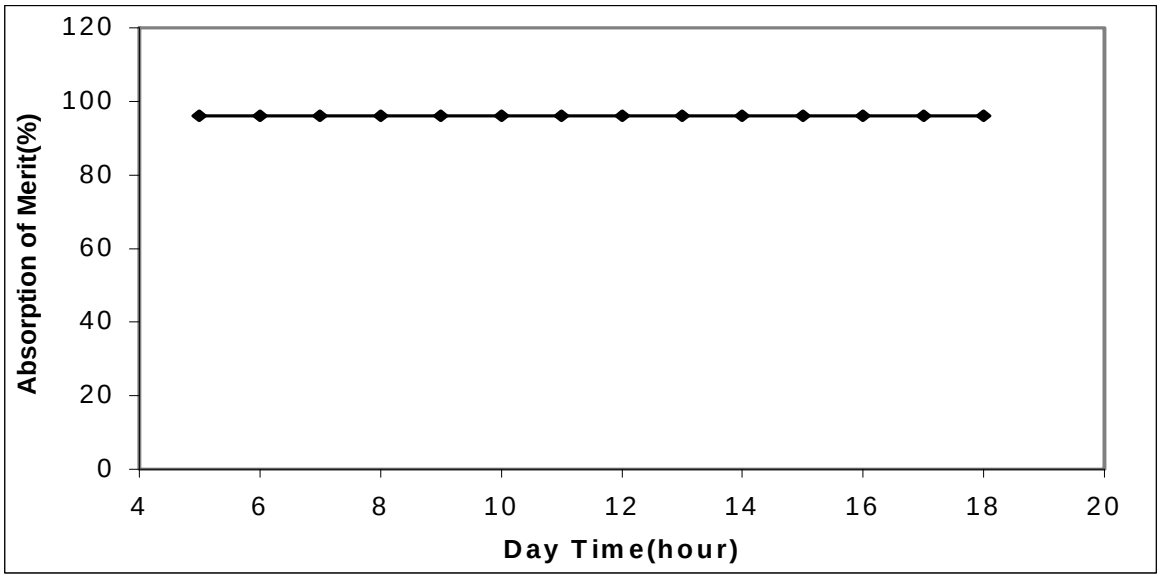


Figure 12. Variation of percent absorption of merit as a function of day time for selective absorber sample of nickel content 82 μg/cm$^2$ sample using prototype A.

Table 4: Accumulative net collective flux (per day) for all samples in different prototypes (A, B, C and D).

| Sample of Nickel Content(±1μg/cm$^2$) | $P_{ac}(A)^1$±1 | $P_{ac}(B)^1$±1 | $P_{ac}(C)^1$±1 | $P_{ac}(D)^1$±1 |
|---|---|---|---|---|
| 0 (Al alloy) | 875 | 851 | 788 | 647 |
| 0 (Cu sheet) | 1125 | 1109 | 1038 | 824 |
| 55 | 5568 | 5566 | 5511 | 4976 |
| 60 | 5586 | 5574 | 5528 | 5017 |
| 70 | 5535 | 5518 | 5469 | 4880 |
| 73 | 5531 | 5455 | 5336 | 4841 |
| 76 | 5516 | 5451 | 5041 | 4631 |
| 80 | 5515 | 5395 | 4953 | 4597 |
| 82 | 5403 | 5395 | 4826 | 4561 |
| 86 | 5300 | 5343 | 4762 | 4402 |
| 92 | 5292 | 5037 | 4713 | 4393 |

[1]Represent the accumulative net collective flux (accumulative net heating power) in different prototypes (A, B, C and D).

For the substrates, the highest value is obtained with copper sheet which gives 1125±1W/m$^2$ in prototype A; while the lowest value is obtained with aluminium alloy which gives 647±1W/m$^2$ in prototype D.

Since each selective absorber sample has a certain nickel content, we will see in the following figures the effect of nickel content on the accumulative collective flux, conversion efficiency and the absorption of merit.

The net collective flux (per day) as a function of the nickel content is shown in figure 13. As the nickel content increased, the accumulative net collective flux is increased to certain nickel content then it decreased after this limit. In other words, there is an optimum value of nickel content that gives the highest accumulative net collective flux.

As we see from figure 13, the nickel content limit is 60μg/cm$^2$. This value is in accordance with the previous study [10].

The average net collective flux (during a day and per hour) for all samples in different prototypes is shown in table 5.

Table 5 is with accordance with table 4 where the highest average net collective flux (during a day and per hour) is obtained for the selective absorber sample of nickel content 60 μg/cm$^2$ which gives 372.4±0.1W/m$^2$ in prototype A; while the lowest value is obtained for the selective absorber of nickel content 92 μg/cm$^2$ which gives 292.9±0.1W/m$^2$ in prototype D.

For the substrates, the highest value is obtained for Cu sample which gives 75.0±0.1 W/m$^2$; while the lowest

value is obtained for aluminium sample which gives 43.1±0.1 W/m$^2$ in prototype D.

The variation of the average net collective flux (during a day and per hour) with the nickel content is shown in figure 14.

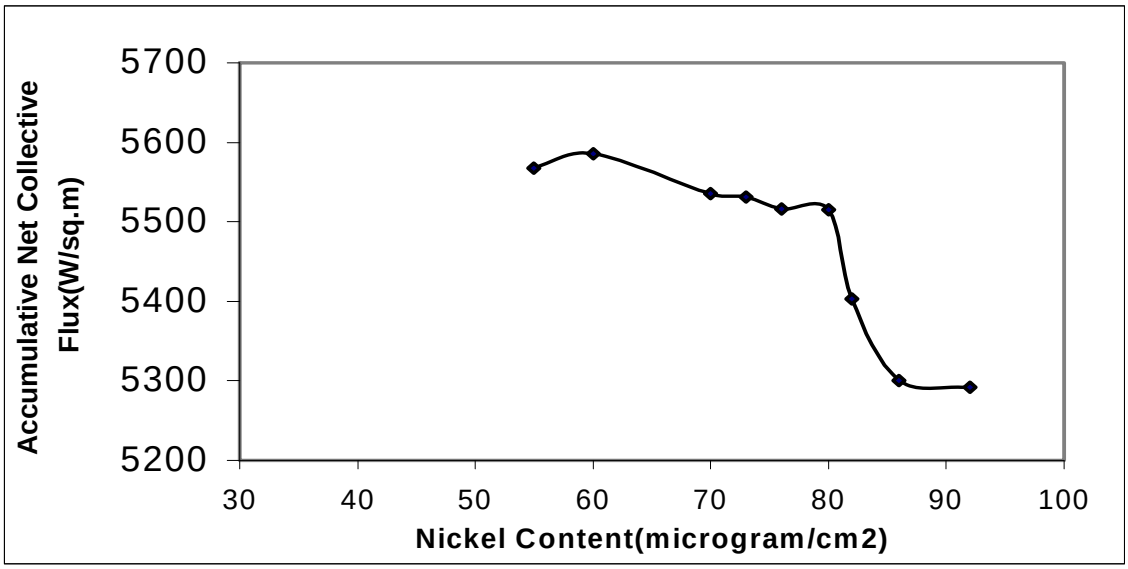


Figure 13. Variation of accumulative net collective flux with the nickel content using prototype A.

Table 5. The average net collective flux (during a day and per hour) for the substrates and the selective absorber samples in different prototypes (A, B, C and D).

| Sample of Nickel Content(±1μg/cm$^2$) | $P_{av}(A)^1$±0.1 | $P_{av}(B)^1$±0.1 | $P_{av}(C)^1$±0.1 | $P_{av}(D)^1$±0.1 |
|---|---|---|---|---|
| 0 (Al alloy) | 58.3 | 56.8 | 52.6 | 43.1 |
| 0 (Cu sheet) | 75.0 | 74.0 | 69.2 | 54.9 |
| 55 | 371.2 | 371.1 | 367.4 | 331.7 |
| 60 | 372.4 | 371.6 | 368.6 | 334.5 |
| 70 | 369.0 | 367.9 | 364.6 | 325.3 |
| 73 | 368.7 | 363.6 | 355.8 | 322.7 |
| 76 | 367.8 | 363.4 | 336.0 | 308.7 |
| 80 | 367.6 | 359.7 | 330.2 | 306.5 |
| 82 | 360.2 | 356.2 | 321.7 | 304.1 |
| 86 | 353.3 | 341.1 | 317.5 | 293.5 |
| 92 | 352.8 | 335.8 | 314.2 | 292.9 |

[1]Represent the accumulative net collective flux (accumulative net heating power) using different prototypes (A, B, C and D).

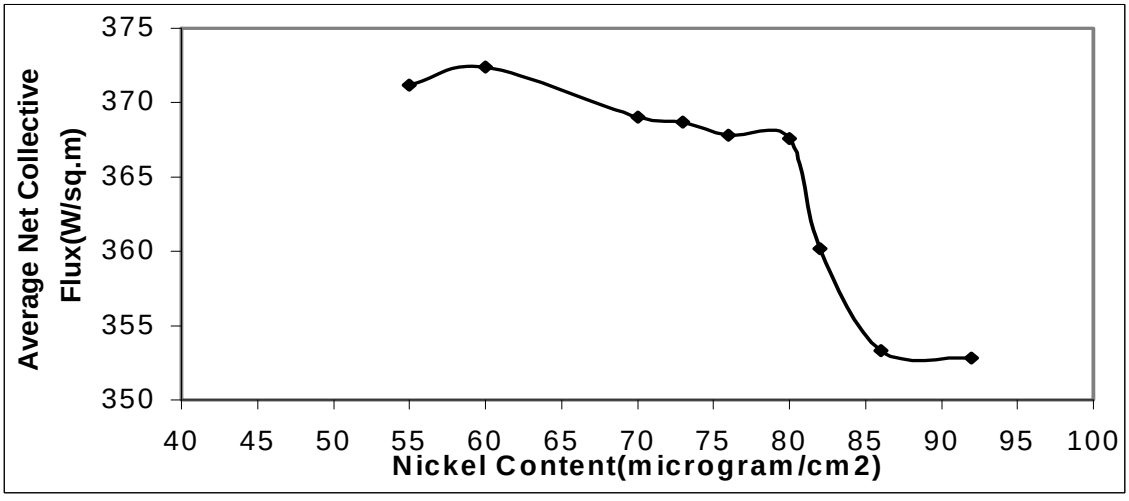


Figure 14: Variation of average net collective flux with the nickel content using prototype A.

Figure 14 is in accordance with figure 13.

The variation of the accumulative net heating power and the average net heating power (for the sample of nickel content 73 μg/cm$^2$ with prototype volume) is shown in figure 15. Linear regression for the accumulative and average net heating power for the sample of nickel content 73 μg/cm$^2$ leads to the following relations:

$\mathbf{P_{ac} = -0.0896\ V + 5551.2}$ with $\mathbf{R^2 = 0.99}$

$\mathbf{P_{av} = -0.0060\ V + 370.1}$ with $\mathbf{R^2 = 0.99}$

Where

$P_{ac}$ is the accumulative net heating power per square meter of the selective absorber during a day.
$P_{av}$ is the average net heating power per square meter of the selective absorber and per hour during a day.
V is the volume of the prototype in cubic centimeter. $R^2$ is the correlation coefficient square.
The above relations represent the accumulative and average net heating power for one sample of nickel content 73 μg/cm$^2$. The accumulative net collective flux is 5551.2 W/m$^2$ and the average net collective flux is 370.1 W/m$^2$, when heat loss is neglected (V = 0.0 cm$^3$).
The extracted relations of the accumulative and average net heating power for nickel pigmented anodized aluminium selective absorber samples are illustrated in table 6 and 7, respectively.

Where

$P_{ac}$ is the net accumulative heating power per square meter of the selective absorber during a day.
V is the volume of the prototype in cubic centimeter.
$R^2$ is the square of the correlation coefficient.

From table 6, the sample of nickel content 60 μg/cm$^2$ is of the highest value. It gives 5656.0 W /m$^2$ , when there is no heat loss (V = 0.0 cm$^3$). However, the lowest value is for sample of nickel content 92 μg/cm$^2$. This sample gives 5151.6 W/m$^2$, when there is no heat loss (V = 0.0 cm$^3$). This value of the nickel content inside the alumina pores is sufficient to grade the refractive index of the layers from the base on aluminium alloy to the top porous alumina layer. Therefore, it gives the optimum selectivity and in turns the maximum solar net collective flux.

The relations can be best described by a linear relationship, because the correlation coefficient square is very close to 0.91 on average.

The relations for all selective absorber samples and substrates are illustrated in table7. Table 7 is in accordance with table 6.
The correlation coefficient squared in the above two tables' shows that the relation between the net heating power and the prototype volume is linear since it is very close to one.
The average percent conversion efficiency is calculated (during a day and per hour) for the substrates and the selective absorber samples as shown in table 8.

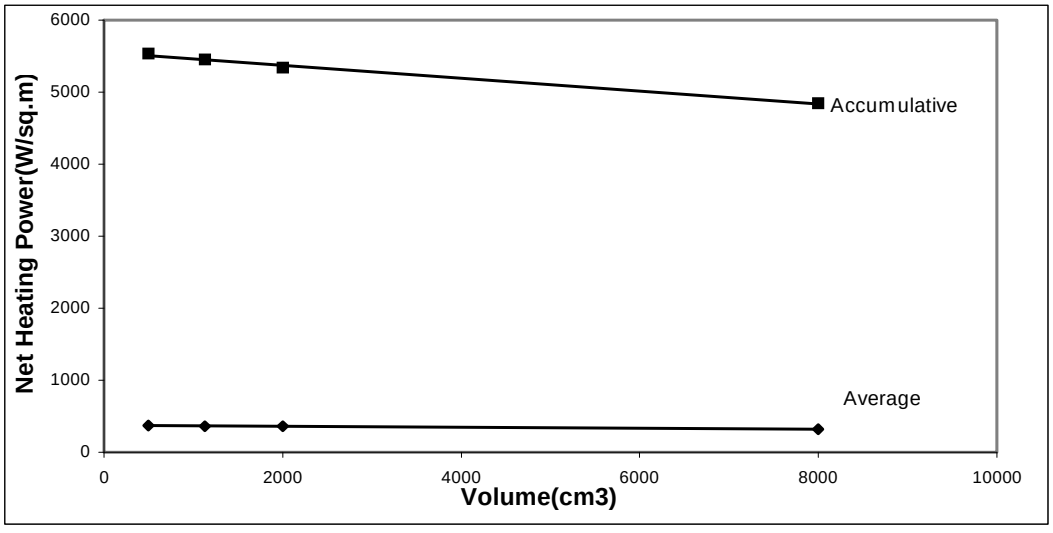


Figure 15. Variation of accumulative and average net heating power for the sample of nickel content 73 μg/cm$^2$ with prototype volume.

Table 6. Extracted relations of the accumulative net heating power for substrates and selective absorber samples during a day.

| Sample of Nickel Content(±1μg/cm$^2$) | Extracted Relation | $R^2$ |
|---|---|---|
| 0 (Al alloy) | $P_{ac}$ = -0.0291 V + 874.8 | 0.97 |
| 0 (Cu sheet) | $P_{ac}$ = -0.0399 V + 1140.0 | 0.99 |
| 55 | $P_{ac}$ = -0.0829 V + 5646.0 | 0.99 |
| 60 | $P_{ac}$ = -0.0790 V + 5656.0 | 0.99 |
| 70 | $P_{ac}$ = -0.0909 V + 5614.5 | 0.99 |
| 73 | $P_{ac}$ = -0.0896 V + 5551.2 | 0.99 |
| 76 | $P_{ac}$ = -0.1109 V + 5482.0 | 0.87 |
| 80 | $P_{ac}$ = -0.1106 V + 5436.5 | 0.82 |
| 82 | $P_{ac}$ = -0.1050 V + 5351.4 | 0.75 |
| 86 | $P_{ac}$ = -0.1173 V + 5292.6 | 0.80 |
| 92 | $P_{ac}$ = -0.1008 V + 5151.6 | 0.80 |

Table 7. Extracted relations of the average net heating power for substrates and selective absorber samples during a day and per hour.

| Sample of Nickel Content(±1μg/cm$^2$) | Extracted Relation | $R^2$ |
|---|---|---|
| 0 (Al alloy) | $P_{av}$ = -0.0019 V + 58.4 | 0.97 |
| 0 (Cu sheet) | $P_{av}$ = -0.0027 V + 76.0 | 0.99 |
| 55 | $P_{av}$ = -0.0055 V + 376.4 | 0.99 |
| 60 | $P_{av}$ = -0.0053 V + 377.1 | 0.99 |
| 70 | $P_{av}$ = -0.0061 V + 374.3 | 0.99 |
| 73 | $P_{av}$ = -0.0060 V + 370.1 | 0.99 |
| 76 | $P_{av}$ = -0.0074 V + 365.5 | 0.87 |
| 80 | $P_{av}$ = -0.0074 V + 362.4 | 0.82 |
| 82 | $P_{av}$ = -0.0068 V + 355.4 | 0.76 |
| 86 | $P_{av}$ = -0.0070 V + 346.7 | 0.84 |
| 92 | $P_{av}$ = -0.0067 V + 343.4 | 0.80 |

Table 8. Average percent conversion efficiency (during a day and per hour) for substrates and selective absorber samples in different prototypes (A, B, C and D).

| Sample of Nickel Content(±1μg/cm$^2$) | $\%\eta_{av}$(A) ± 0.1[1] | $\%\eta_{av}$ (B) ± 0.1[2] | $\%\eta_{av}$ (C) ± 0.1[3] | $\%\eta_{av}$ (D) ± 0.1[4] |
|---|---|---|---|---|
| 0 (Al alloy) | 12.5 | 11.0 | 13.0 | 12.0 |
| 0 (Cu sheet) | 15.0 | 15.5 | 17.0 | 12.8 |
| 55 | 72.0 | 74.0 | 72.0 | 65.0 |
| 60 | 72.0 | 74.0 | 73.0 | 73.2 |
| 70 | 72.0 | 73.0 | 72.0 | 64.0 |
| 73 | 72.0 | 73.0 | 72.0 | 64.0 |
| 76 | 71.0 | 72.0 | 72.0 | 61.0 |
| 80 | 71.0 | 71.0 | 72.0 | 61.0 |
| 82 | 69.0 | 68.0 | 71.0 | 61.0 |
| 86 | 69.0 | 68.0 | 71.0 | 61.0 |
| 92 | 69.0 | 68.0 | 68.0 | 61.0 |

Where : [1]Average percent conversion efficiency using prototype A. [2]Average percent conversion efficiency using prototype B. [3]Average percent conversion efficiency using prototype C. [4]Average percent conversion efficiency using prototype D.

Table 8 shows that the highest average percent conversion efficiency (during a day and per hour) obtained is (74.0±0.1)%, and the lowest value is (61.0±0.1)% for different selective absorber samples in different prototypes.

For the substrates, the highest value is obtained with Copper substrate which is (17.0±0.1)%, while the lowest value is obtained with Aluminium alloy substrate which is (11.0±0.1)%.

From table 8, the maximum net collective flux obtained is (699.2±0.1)W.m2 for sample of nickel content 60 μg/cm2 using prototype A; while the lowest value is (590.3±0.1)W.m2 for sample of nickel content 92 μg/cm$^2$ using prototype D.

Concerning substrates, the maximum value obtained is (138.4±0.1) W.m$^2$ for Cu sheet using prototype A; while the lowest value obtained is (89.4±0.1) W.m$^2$ for Al alloy in prototype D.

The relation between the maximum net collective fluxes (during a day) with prototype volume (for one sample of nickel content 73 μg/cm$^2$) is shown in figure 16.

The relation between the maximum net collective fluxes with prototype volume is given by:

$P_{max} = -0.0072\ V + 676.0$ with $R^2 = 0.99$

The relations for all selective absorber samples are illustrated in table 9.

These relations are fall in the interval time 11:00 to 13:00 during a day.

The effect of the nickel content on the maximum net collective flux obtained during a day is shown in figure 18.

The variation of the maximum net collective flux with nickel content in figure 15 has the same behavior as in previous figures.

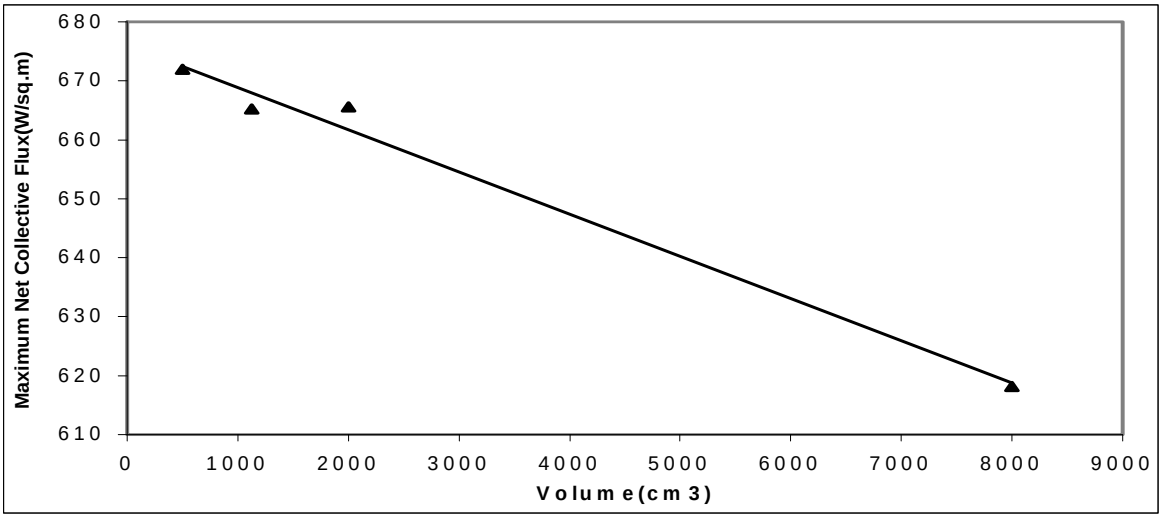


Figure 16. Variation of the maximum net collective flux with prototype volume for sample of nickel content 73 μg/cm$^2$.

Table 9. Extracted relations of the maximum net heating power for the selective absorber samples during a day.

| Sample of Nickel Content(±1μg/cm$^2$) | Extracted Relation | $R^2$ |
|---|---|---|
| 55 | $P_{max} = -0.0064\ V + 683.2$ | 1.00 |
| 60 | $P_{max} = -0.0071\ V + 694.6$ | 0.93 |
| 70 | $P_{max} = -0.0063\ V + 679.2$ | 0.97 |
| 73 | $P_{max} = -0.0072\ V + 676.0$ | 0.99 |
| 76 | $P_{max} = -0.0074\ V + 669.6$ | 0.96 |
| 80 | $P_{max} = -0.0073\ V + 662.4$ | 0.83 |
| 82 | $P_{max} = -0.0069\ V + 657.5$ | 0.75 |
| 86 | $P_{max} = -0.0060\ V + 638.4$ | 0.91 |
| 92 | $P_{max} = -0.0055\ V + 632.1$ | 0.81 |

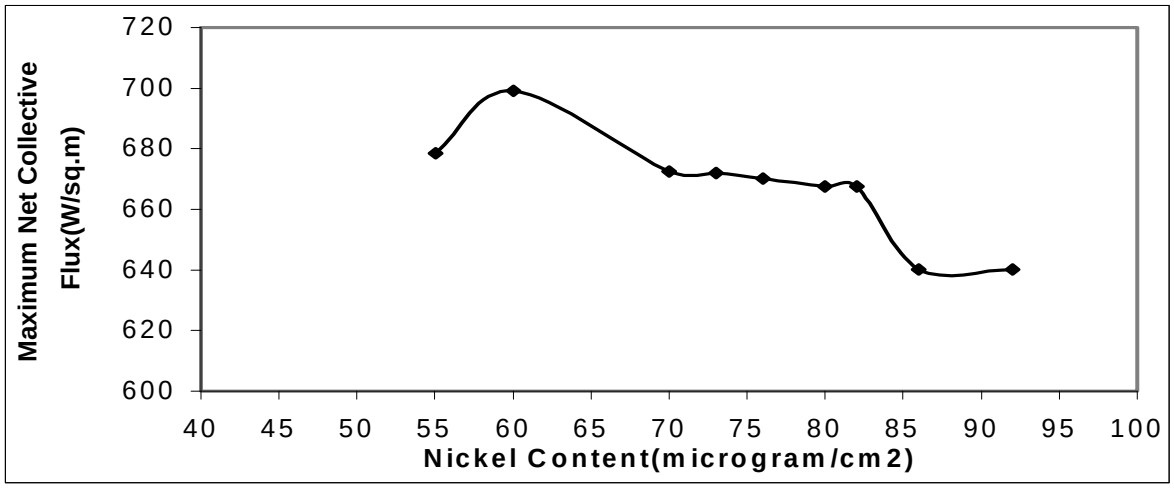


Figure 17.Variation of maximum net collective flux obtained during a day with the nickel content using prototype A.

## 5. Conclusions

Nickel pigmented anodized aluminium alloy selective absorbers prepared by dc anodization (using dilute phosphoric acid) followed by electrolysis in nickel sulphate solution (coloration) using ac and prc currents were used.

The substrates and the selective absorber samples are tested at Bethlehem University at a horizontal level where certain experimental set-up is used. The substrates selective absorber samples were tested inside prototypes of volume in the range of 500–8000±1cm$^3$.

The net heating power (net collective flux) (average, accumulative and maximum), conversion efficiency (average and maximum) and absorption of merit (average and maximum) were studied.

Comparing aluminium alloy with copper sheet shows that copper sheet gives higher net collective flux, conversion efficiency and absorption of merit than aluminium alloy.

Prototype of volume 500±1 cm$^3$ is of the most suitable prototype because it has the least conduction-convection losses. The highest conversion of the solar flux is found for the selective absorber of nickel content 60 μg/cm$^2$. However, the lowest conversion of the solar energy into thermal energy is found for sample of nickel content 92μg/cm$^2$ due to its high emissivity.

The effects of nickel content, in the alumina pores, on the converted solar flux is that as the nickel content increased the absorptivity is increased. However, there is a nickel content limit that gives the optimum net collective flux and selectivity. This limit is 60μg/cm$^2$.This limit of nickel content is sufficient to decrease the refractive index gradually from the barrier alumina (at the bottom) to the upper porous alumina. Therefore the solar radiation can be trapped inside the alumina pores that have certain nickel content (nickel particles). This trapping gives good opportunity for the radiation to be absorbed by multi reflection of the radiation inside the pores and by the resonant scattering of radiation among nickel particles embedded in the alumina pores (figure2).There is a linear relationship between the net heating power (collective flux) (average, accumulative and maximum) and average absorption of merit with prototype volume.

The commercial polyethylene is used because it is a good shield for glazed insulated prototype reduces the connective loss and protects the selective absorber against degradation.

## References

[1] C.M. Lampert, Solar Energy Materials Vol. 1, 1979, 319.

[2] Sten Löfving, Solar Energy Materials Vol. 5, 1981, 103.

[3] C.M. Lampert, Solar Energy Materials Vol.2, 1979, 1.

[4] C.G. Granqvist, Physica Scripta. , Vol. 32, 1985, 401.

[5] A. Wazwaz, PhD Thesis, Paul Sabatier, Toulouse, France, 2001.

[6] M.S. Sodha, S.S. Mathur and M.A.S. Malik, "Reviews of Renewable Energy Resources", John Wiley and Sons, Vol. 2, 1983, 237- 239 and 297-319.

[7] A.S. Elasfouri and M. M. Hawas, Energy Convers. Mgmt Vol. 27, No. 1, 1987, 1.

[8] H.C. Hottel and A. Whillier, "Evaluation of flat-plate solar collector performance", Trans. Of Conference on the Use of Solar Energy, University of Arizona 2, 1958, 74.

[9] P.K. Gogna, S. C. Mullick and K.L. Chopra , Int. J. Energy Research, Vol. 4, 1980, 317.

[10] J .Salmi, "Elaboration Et Caracterisation De Couches Absorbante Selectives Solaires Sur L'Alliage D'Aluminium 1050", Thesis, Paul Sabatier University, Toulouse, France 1999.

[11] A. Abene, V. Dobois, M. Le Ray and A. Ouagued, Journal of Food Engineering, Vol. 1, No. 65, 2004, 15.

[12] K. Srithar, A. Mani, Journal of Zhejiang University Science A, Vol. 11, No. 7, 2006, 1870.

[13] Sia, Toh Ching, Velautham, Sanjayan, Darus, and Amer Nordin, International Energy Journal, Vol. 8, No. 2, 2007, 125.

[14] S.A. Kalogirou, S. Lalot, G. Florides, and B. Desmet, Solar Energy, Vol. 2, No. 82, 2008, 164.

[15] D. Kruger, Y. Pandian, K. Hennecke, and M. Schmitz, Desalination, 1-3(220), 612(20.